most polymer melts. The spin-lattice relaxation process of protons in poly(dimethylsiloxane)[27] exhibits no variations when the chain molecular weight is higher than 3×10^3, whereas the resonance line width observed on the same polymer may vary from about 1 to about 10^2 Hz when the chain molecular weight goes from 10^3 to 2×10^6. More important is the qualitative change of the transverse spin-system response induced by increasing the chain molecular weight and going from a liquid response to a solidlike one, determined by strong entanglement of long chains. The longitudinal relaxation is only sensitive to local motions of monomer units, occurring around the Larmor frequency (2×10^8 rad·s^{-1}); these are generally independent of the chain molecular weight. The transverse magnetization dynamics is mainly sensitive to long-range motions involving the terminal chain diffusional spectrum; this corresponds to low relaxational frequencies and strongly depends upon the chain molecular weight. The presence of entanglements originates a residual energy of dipole-dipole interactions of nuclei; this energy expressed in frequency units was used as an internal reference throughout the present paper to characterize the terminal spectrum of chain diffusion in a melt.

Several features result from the present NMR investigation of fractionated PDMS samples:

(i) The best agreement with experimental results is obtained by assuming that a macromolecule in a melt loses the memory of its organization in space at every part of the chain, at any time; the resulting multiple-relaxation mode is characterized by a terminal relaxation time whose molecular weight dependence is proportional to $\bar{M}_w^{3.4\pm0.3}$; it is equal to about 3 s for $\bar{M}_w \sim 1.0 \times 10^6$ at room temperature.

(ii) Measurements performed both on ^{13}C and ^{1}H nuclei gave similar results; since ^{13}C nuclei in natural abundance have no interchain interactions, we consider that single-chain magnetic properties are perceived from ^{13}C nuclei, although all chains are in dynamical interactions with one another.

(iii) Finally, high-speed sample rotation clearly shows that effects of the residual dipole-dipole interactions are progressively screened by increasing the rate of chain disentanglement.

Acknowledgment. Poly(dimethylsiloxane) samples were fractionated and characterized by M. Sauviat.

References and Notes

(1) De Gennes, P. G. *J. Chem. Phys.* **1971**, *55*, 572.
(2) Doi, M.; Edwards, S. F. *J. Chem. Soc., Faraday Trans. 2* **1978**, *74*, 1789.
(3) Doi, M.; Edwards, S. F. *J. Chem. Soc., Faraday Trans. 2* **1979**, *74*, 1802.
(4) Bueche, F.; Cashin, W.; Debye, P. *J. Chem. Phys.* **1952**, *20*, 1956.
(5) Klein, J. *Macromolecules* **1981**, *14*, 460.
(6) Leger, L.; Hervet, H.; Rondelez, F. *Macromolecules* **1981**, *14*, 1334.
(7) De Gennes, P. G. *Macromolecules* **1976**, *9*, 587.
(8) Callaghan, P. T.; Pinder, D. N. *Macromolecules* **1984**, *17*, 431.
(9) Cohen Addad, J. P. *J. Chem. Phys.* **1979**, *71*, 3689.
(10) Cohen Addad, J. P. *J. Phys. (Les Ulis, Fr.)* **1982**, *43*, 1509.
(11) Cohen Addad, J. P.; Feio, G. *J. Polym. Sci., Polym. Phys. Ed.* **1984**, *22*, 957.
(12) Cohen Addad, J. P.; Guillermo, A. *J. Polym. Sci., Polym. Phys. Ed.* **1984**, *22*, 931.
(13) Rouse, P. E. *J. Chem. Phys.* **1953**, *21*, 1272.
(14) Cohen Addad, J. P. *Polymer* **1983**, *24*, 1128.
(15) Graessley, W. W.; Edwards, S. F. *Polymer* **1981**, *22*, 1329.
(16) Graessley, W. W. *Adv. Polym. Sci.* **1982**, *47*, 67.
(17) Pake, G. *J. Chem. Phys.* **1948**, *16*, 327.
(18) Andrew, E. R.; Bersohn, R. *J. Chem. Phys.* **1950**, *18*, 159.
(19) Abragam, A. "Principles of Nuclear Magnetism", Oxford University Press: London, 1961.
(20) Cohen Addad, J. P.; Roby, C. *J. Chem. Phys.* **1975**, *65*, 3091.
(21) English, A. D.; Dybowski, C. R. *Macromolecules* **1984**, *17*, 446.
(22) Cohen Addad, J. P.; Domard, M.; Lorentz, G.; Herz, J. *J. Phys. (Les Ulis, Fr.)* **1984**, *45*, 575.
(23) De Gennes, P. G. "Scaling Concepts in Polymer Physics"; Cornell University Press: Ithaca, NY, 1979.
(24) Ferry, J. D. "Viscoelastic Propertis of Polymers", 3rd ed; Wiley: New York, 1980.
(25) Kataoka, T.; Veda, S. *Polym. Lett.* **1966**, *4*, 317.
(26) Powles, J. G.; Hartland, A.; Kail, J. A. E. *J. Polym. Sci.* **1961**, *55*, 361.
(27) Cunniberti, C. *J. Polym. Sci., Part A-2* **1970**, *8*, 2051.

Trends in Molecular Motion for a Series of Glucose Oligomers and the Corresponding Polymer Pullulan As Measured by ^{13}C NMR Relaxation

Alan J. Benesi* and David A. Brant

Department of Chemistry, University of California, Irvine, California 92717.
Received September 28, 1984

ABSTRACT: The dipolar ^{13}C relaxation parameters T_1, T_2, and NOE have been measured at 62.83 MHz for a series of glucose oligomers and the corresponding high molecular weight, linear polymer pullulan. Significant chemical shift differences made it possible to differentiate between ^{13}C atoms in terminal glucose rings, penultimate glucose rings, and interior glucose rings of the oligomers. Terminal and penultimate ring atoms exhibit consistently higher values of T_1, T_2, and NOE than do interior ring atoms. For each type of ring the ^{13}C relaxation parameters approach a characteristic asymptotic limit at about DP = 12. The relaxation parameters of interior ring ^{13}C atoms in the oligomers match those of pullulan at a critical DP = 15. This indicates that the relative angular motion of interior ^{13}C magnetic moments and their directly bonded ^{1}H magnetic moments generates the same electromagnetic power at the pertinent magnetic resonance frequencies, and suggests that the underlying atomic motion is the same in both cases.

Introduction

In addition to its other uses, NMR spectroscopy can serve as a probe of solute motion in liquid solutions. Pulsed-field gradient NMR spectroscopy can be used to measure the translational diffusion coefficients of solute molecules,[1,2] while quadrupolar NMR relaxation measurements and ^{13}C NMR relaxation measurements provide information on the details of the rotational diffusion of

0024-9297/85/2218-1109$01.50/0

solute molecules.[3-5] All three of these NMR techniques have been applied successfully, but the anisotropy of molecular motion greatly complicates analysis of the data from the latter two techniques.

Relaxation measurements with ^{13}C are sensitive to rotational motion, because ^{13}C relaxation is predominantly dipolar at currently available magnetic field strengths (below about 12 T) if there are directly bonded H atoms.[4] In this case the ^{13}C relaxation parameter measured (T_1, T_2, or NOE) for a given resonance line depends on the random angular motion of the corresponding ^{13}C–^1H bond vector(s), with the magnitudes of T_1 and T_2 inversely proportional to the number of directly bonded H atoms. Thus, if there are differences in the angular motion of different carbon atoms in a molecule, different relaxation parameters will be observed for the corresponding resonance lines. This circumstance may be used to differentiate between more and less mobile ^{13}C atoms within a molecule.[6-11]

The exact relationship between dipolar relaxation and molecular motion involves the spectral density of the electromagnetic power generated by the relative motion of the ^{13}C and ^1H nuclear magnetic moments at the resonance frequencies of both ^{13}C and ^1H, and at certain combinations (harmonics) of these frequencies (including the power at low frequencies, ~0 Hz, which contributes to T_2). Since different types of anisotropic motion can generate the same spectral density at these specific frequencies, matching a model of anisotropic motion to the observed relaxation parameters does not guarantee that the model is correct, even if the relaxation parameters are determined over a wide range of frequencies.[10-12]

A direct way to gain an understanding about solute molecular motion without using a model is to compare dipolar ^{13}C relaxation parameters for ^{13}C nuclei in the same molecule. In this way the relative motion of the several carbon atoms can be compared, but there is no attempt to choose a model. This method has been widely used for oligomers and polymers, where the relaxation parameters of chain-end, branch-group, and main-chain carbon atoms are usually different.[6-11]

Related to this is the dependence of ^{13}C dipolar relaxation parameters on the molecular weights of random-coil polymers in dilute solution.[11] Above a fairly small critical molecular weight or degree of polymerization (DP), the relaxation parameters are independent of chain length, because of the dominant contribution of "segmental motion" to the spectral power density.[11] In a small rigid molecule the relative atomic motions of all carbon atoms and their respective attached hydrogen(s) follow the motion of the molecule as a whole. For such molecules in the extreme narrowing limit the ^{13}C relaxation parameters, T_1, T_2, and NOE, decrease with increasing molecular weight as the rotational diffusion coefficient decreases.[3-5] For a large flexible molecule the relative atomic motion of a particular carbon atom and its attached hydrogen atom(s) is determined by the motion of that part of the molecule in which the atom is located. Such localized atomic motions are referred to as segmental motions[11] to communicate the idea that atoms rigidly connected to an atom of interest tend to have similar atomic motions and therefore that those ^{13}C atoms within a given inflexible segment of the larger molecule will have similar ^{13}C relaxation parameters. In a homologous series of molecules with increasing molecular weights the critical molecular weight (or DP) occurs when control of ^{13}C dipolar relaxation shifts from overall molecular motion, which depends on the molecular weight, to segmental motion, which does not. A critical molecular weight has been observed for many synthetic polymers in dilute solution.[11] Segmental motion is also known to dominate relaxation in random-coil polysaccharides,[13,14] but the critical molecular weight has not previously been reported for any polysaccharide.

The critical DP reported for various synthetic polymers varies from 30 for poly(ethylene oxide) in D_2O to 400 for poly(dimethylsiloxane) in tetrachloroethene.[11] The relaxation parameters are essentially independent of concentration up to 10–15 monomer mol % for random-coil synthetic polymers, which indicates that the segmental motion of these polymers is unaffected by intermolecular effects below this concentration level.[11]

Here we report trends with DP in the ^{13}C relaxation parameters for the linear, unbranched polysaccharide pullulan, which is believed to adopt a random-coil configuration in aqueous solution,[15,16] and for a series of glucose oligomers which asymptotically approach pullulan in structure and dynamics. Pullulan is a high molecular weight extracellular α-D-glucan produced by the organism *Aureobasidium pullulans*.[17] Whereas amylose, the linear component of starch, is a homopolymer of α-1,4-linked D-glucose, pullulan has the same structure with every third α-1,4-linkage replaced by an α-1,6-linkage. Pullulan is an amorphous polymer readily soluble in water, while amylose is partially crystalline and displays only limited aqueous solubility. These differences are presumably related in part to the greater conformational freedom inherent in the α-1,6-linkages.[15]

The enzyme pullulanase is an endoglycosidase specific for hydrolysis of α-1,6-linkages. Its action on pullulan produces linear fragments consisting predominantly of maltotriose (G_3), which contains two α-1,4-linkages, and the α-1,6-linked hexameric, nonameric, dodecameric, etc., oligomers of maltotriose denoted here by $(G_3)_2$, $(G_3)_3$, $(G_3)_4$, etc., respectively.[18] At least some of the ^{13}C resonance signals for each oligomer can be positively assigned on the basis of chemical shifts to a particular glucose ring in the chain and to a particular carbon atom within that ring.[19-21] The ^{13}C resonances of different rings have not only different chemical shifts, but also different relaxation parameters. Trends in the relaxation parameters of terminal rings, penultimate rings, and interior rings can thus be measured as a function of the DP of the oligomer.

Experimental Section

D-Glucose (Mallinckrodt AR), D-(+)-maltose (Aldrich), maltotriose (Aldrich), maltotetraose (obtained from Dr. John Robyt, Iowa State University), and pullulan ($M_n = 6.2 \times 10^4$ and $M_n = 66.1 \times 10^4$, Hayashibara Biochemical Laboratories, Okayama, Japan) required no purification prior to NMR sample preparation. Oligomers $(G_3)_2$, $(G_3)_3$, $(G_3)_4$, and $(G_3)_5$ of the three-membered repeat unit were produced by pullulanase-catalyzed hydrolysis of the lower molecular weight pullulan. From 0.7 to 1.0 g of pullulan was dissolved in 4 mL of Millipore Milli-Q water; then 0.07–0.20 mL of pullulanase (*Enterobacter aerogenes*, E.C. No. 3.2.1.9, Calbiochem-Behring, 83 units/mL) solution in Milli-Q water was added, and hydrolysis was allowed to proceed at room temperature for 2–8 h. No pH adjustment was necessary, since the reaction mixture was about pH 5, close to the pH of optimal activity for pullulanase.[18] After reaction the mixture was applied with a syringe pump to a 2.5 cm i.d., 1 m column, packed to a depth of 83 cm with Bio-Gel P4 (Bio-Rad Laboratories, 200–400 mesh wet). The jacketed column was maintained at 64 °C and eluted with Milli-Q water.[22,23] The effluent was monitored at 206 nm with a UV monitor (LKB 2138 Uvicord S), and 5-mL fractions were collected on an LKB 2111 Multirac fraction collector. This procedure gave sharp separation of oligomers between 3 and 18 glucose units in chain length. Fractions of equal DP were saved, combined, freeze-dried, and sometimes rechromatographed until sufficient chromatographically pure freeze-dried oligomer was

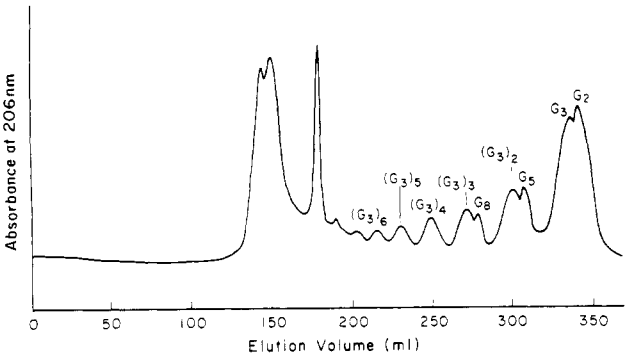

Figure 1. Separation of oligosaccharides produced by the pullulanase-catalyzed hydrolysis of pullulan.

obtained for NMR experiments (at least 0.20 g). The pH of all aqueous monomer (glucose), oligomer, and polymer samples was between 6 and 7 prior to freeze-drying.

All NMR samples were prepared from the pure compounds in the following way. The pure solid was dissolved in D_2O (Aldrich Gold Label) and then freeze-dried in order to replace exchangeable hydrogen atoms with deuterium. A 5% (w/w) solution in D_2O was then prepared except for the $(G_3)_5$ for which a 3.5% (w/w) solution was prepared because of the limited quantity available. Each solution also contained 0.02% sodium azide as preservative. The 5% solution was then filtered through a 0.45-μm Millipore filter into a 10-mm NMR tube. This tube was sealed after five freeze–pump–thaw cycles. All ^{13}C T_1 measurements were performed by using the inversion–recovery method with a pulse sequence π-variable delay–$\pi/2$-fixed delay (at least $5 \times T_1$ of the most slowly relaxing peak) at 62.83 MHz in a Bruker WM-250 spectrometer with complete noise decoupling of protons. The ^{13}C T_2 measurements were performed by the Carr–Purcell–Meiboom–Gill method with phase alternation,[24] again with complete noise decoupling of the protons. (A correction for the effect of noise decoupling on the measured T_2[25] is discussed in the next section.) The ^{13}C NOE's were evaluated from the ratios of peak intensities with complete decoupling to those obtained when noise decoupling was "gated" on 2 ms before pulse and acquisition; peak crowding made integrals unreliable. Noise decoupling was switched off for $10 \times T_1$ of the most slowly relaxing peak prior to the pulse.[26] The magnetic field was locked on the deuterium resonance. Chemical shifts were measured relative to an external solution of dioxane in D_2O in a separate 10-mm tube. All measurements were carried out at 30 °C. Each T_1 and T_2 experiment required an overnight run of 8–10 h; the number of transients collected at each delay time was governed by the required relaxation delay ($5 \times T_1$ of the most slowly relaxing peak).

Results and Discussion

The oligomers $(G_3)_n$ were prepared by enzymatic hydrolysis of pullulan as described in the Experimental Section. The extent of hydrolysis determined the relative amounts of the several oligomers recovered. A typical record of the distribution of oligomers obtained after gel exclusion chromatography of a pullulan hydrolysis mixture is shown in Figure 1. Enzyme and partially hydrolyzed pullulan elute earlier than the smaller oligomers, which appear at times related inversely to their molecular weights. The peaks of the smaller pullulan oligomers often consisted of two overlapping peaks, indicating that not only the anticipated 3-, 6-, and 9-mers were present, but also 2-, 5-, and 8-mers. The quantities of these secondary oligomers were significant, but it is not clear how they arose. Possibilities include an intrinsic α-1,4-glucan hydrolase activity in pullulanase, traces of α-1,4-glucan hydrolase impurity in the pullulanase, a broad distribution of pullulan molecular weights with many short chains and a correspondingly high frequency of chain ends not terminating in maltotriose units, or even a natural occurrence of maltose (G_2) units interspersed among the predominant maltotriose repeat units. Complete pullulanase-catalyzed hydrolysis of high molecular weight pullulan with a different batch of the enzyme yielded maltotriose exclusively in an earlier unpublished study. This and the ^{13}C NMR spectrum of pullulan[21] militate against the final possibility. In any case, the secondary oligomers were separated from the desired oligomers $(G_3)_n$ by rechromatography when necessary. The identities of the oligomers $(G_3)_n$ were verified from their ^{13}C NMR spectra.

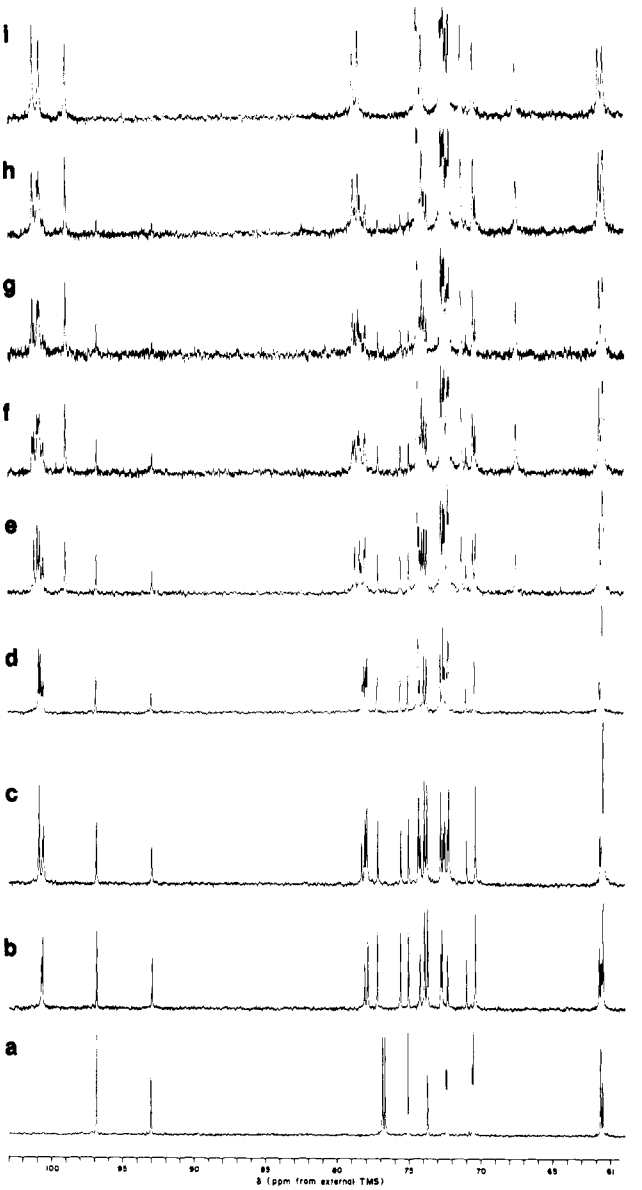

Figure 2. ^{13}C NMR spectra of (a) glucose (G), (b) maltose (G_2), (c) maltotriose (G_3), (d) maltotetraose (G_4), (e) $(G_3)_2$, (f) $(G_3)_3$, (g) $(G_3)_4$, (h) $(G_3)_5$, and (i) pullulan.

The ^{13}C NMR spectra of the series of pullulan oligomers are shown in Figure 2. The molecules glucose, maltose, maltotriose, $(G_3)_2$, $(G_3)_3$, $(G_3)_4$, and $(G_3)_5$ are part of the series of molecules which lead to pullulan in the limit of long chain length. The molecule maltotetraose (G_4) is the only oligomer which does not fit in this series. It has three α-1,4-linkages rather than two α-1,4-linkages followed by an α-1,6-linkage. It was included in this study for purposes of comparison.

The ^{13}C chemical shift assignments are shown in Figure 3. Peak assignments are based on literature values for glucose, maltose, maltotriose, panose, and pullulan.[19-21] The complete assignment of peaks for maltotriose[19,20] was particularly helpful, because peaks which appeared for the 6-mer that did not appear in maltotriose were obvious.

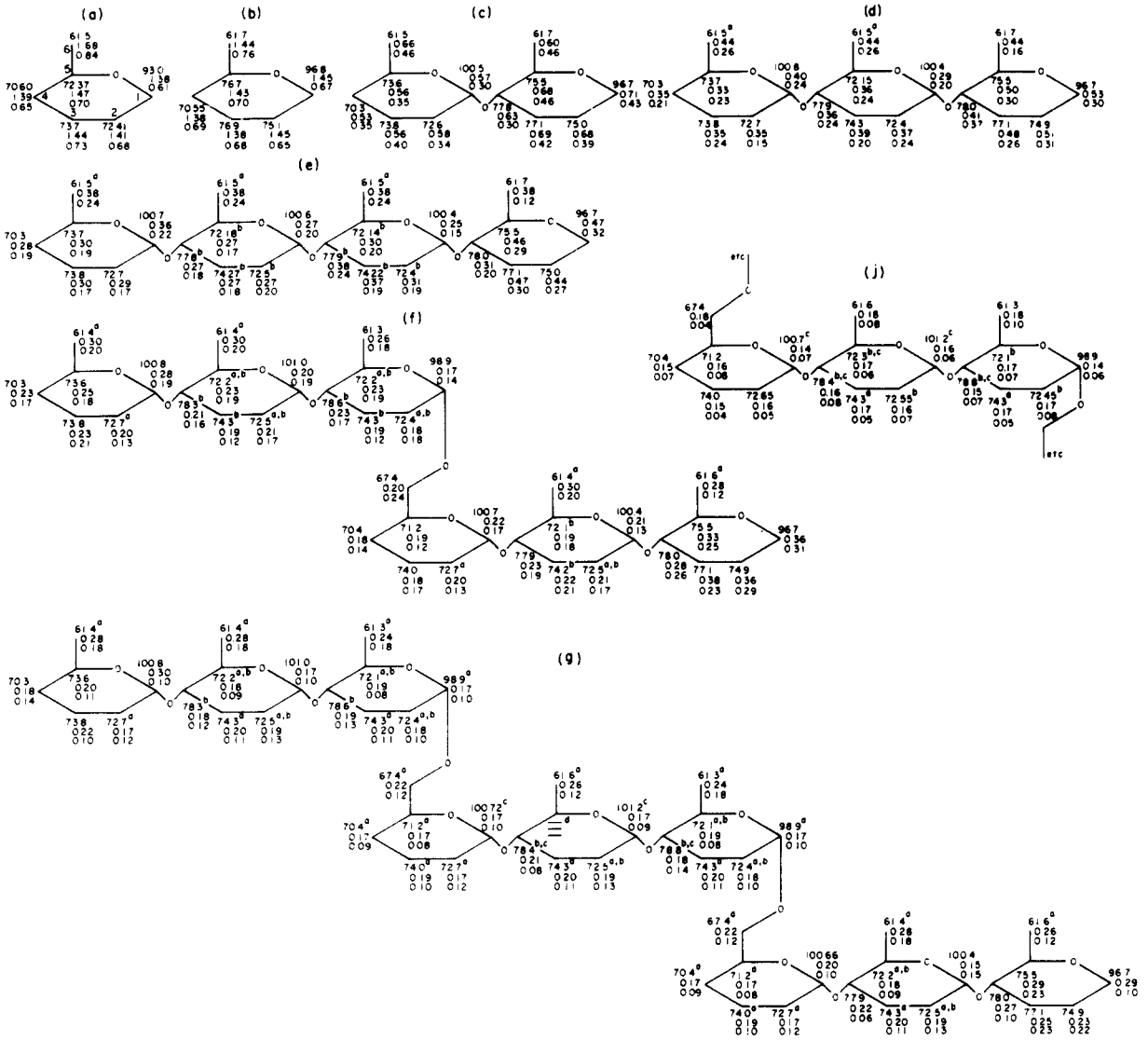

Figure 3. Chemical shift (δ), NT_1, and NT_{2exptl} values as a function of carbon atom location within the various molecules: (a) α-glucose, (b) β-glucose, (c) maltose (G_2), (d) maltotriose (G_3), (e) maltotetraose (G_4), (f) $(G_3)_2$, (g) $(G_3)_3$, (h) $(G_3)_4$, (i) $(G_3)_5$, (j) pullulan. The top number is δ in ppm from Me_4Si, the middle number is NT_1 in seconds, and the bottom number is NT_{2exptl} in seconds. A superscript a next to the chemical shift indicates that other carbon atoms in the molecule share the same parameters. A superscript b indicates

These, in turn, could be used to identify most of the peaks for the 9-mer, 12-mer, 15-mer, and ultimately pullulan itself. For example, the ^{13}C resonance furthest downfield at 101.2 ppm (relative to external Me_4Si) does not appear in the maltotriose or 6-mer spectra, but does appear in the 9-mer, 12-mer, 15-mer, and pullulan spectra. In the 9-mer it must therefore represent C(1) of one of the three interior glucose rings of the chain. It cannot be $C(1)_4$ (ring carbon C(1) in ring number 4 counting from the reducing end), because this resonance and that of $C(1)_7$ occur at 98.9 ppm corresponding to a C(1) involved in an α-1,6-linkage.[20] It cannot represent $C(1)_6$, because this resonance should occur about 1.7 ppm downfield from the C(1) resonances of rings 4 and 7.[21] Therefore, it must represent $C(1)_5$ in an environment that appears for the first time in $(G_3)_3$.

Peak integrals were also useful in assignments, although variable NOE's for different resonances (see paragraph at end of text regarding supplementary material) in longer chain oligomers complicate interpretation on this basis. Both ^{13}C T_1 and T_2 values were also helpful in confirming peak assignments, because interior rings usually had shorter T_1's and T_2's than terminal rings. (See Figure 3, where, to compensate for the numbers N of hydrogens directly bonded to each carbon, relaxation times are reported as NT_1 and NT_2.)

Not all peaks could be positively assigned to a specific $C(m)_n$ atom, where m is the carbon atom number within a given glucose unit and n is the glucose unit ring number with the reducing terminal ring assigned $n = 1$. Twelve intense spectral lines are observed for glucose, 20 for maltose, 24 for maltotriose (G_3), 35 for $(G_3)_2$, 40 for $(G_3)_3$ and $(G_3)_4$, 38 for $(G_3)_5$, and 18 for pullulan (see Figure 2). Some of these lines are not recorded in Figure 3, where only the data for the predominant β-anomeric forms of the oligomers are reported. Assignments of all observed peaks appear in the supplementary material. Shoulder peaks and

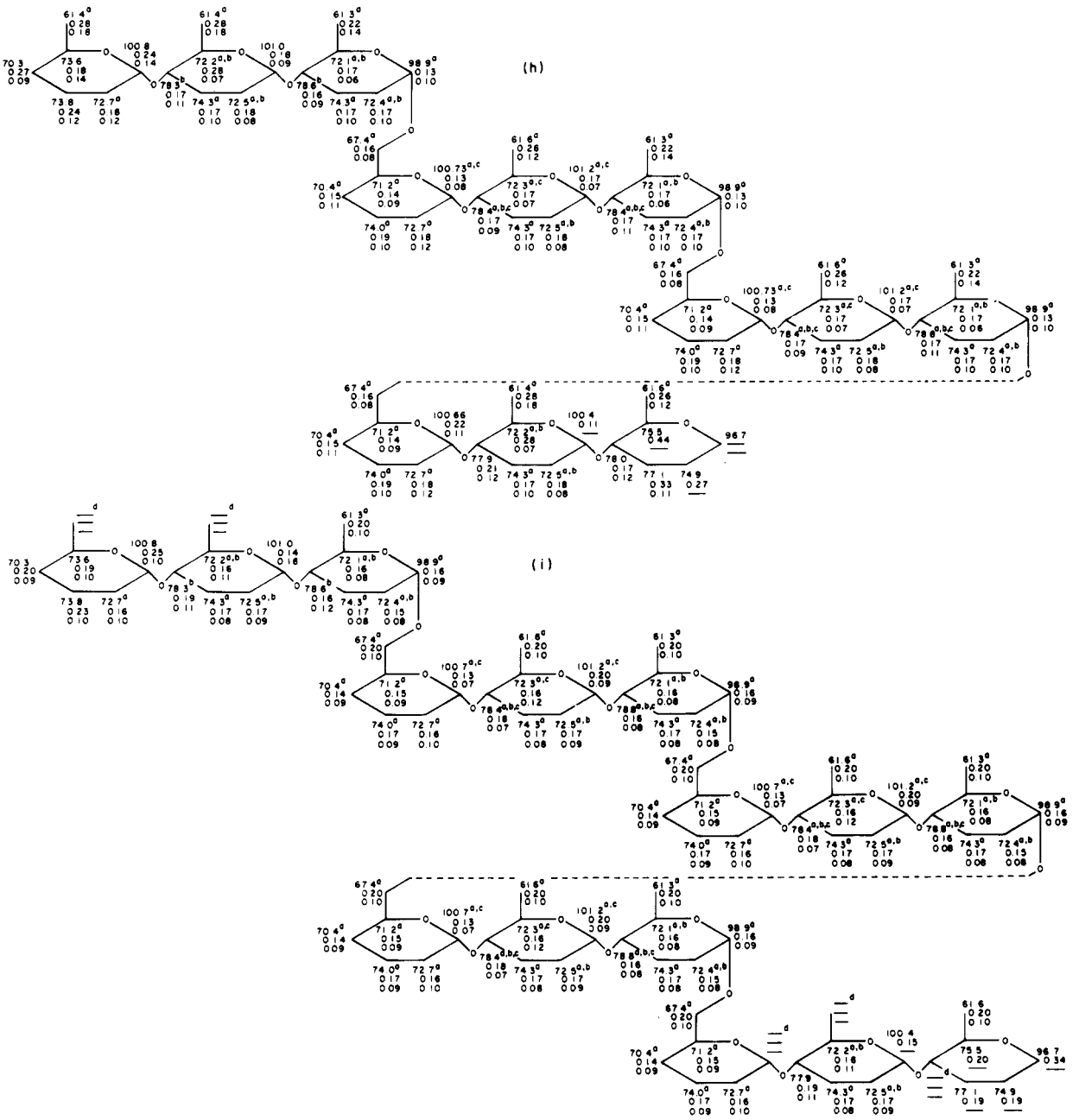

that the assignment is ambiguous and may be exchanged with the assignment for another carbon atom that has a similar chemical shift. A superscript c designates an interior carbon. A superscript d denotes a peak which is barely discernible and for which no data could be obtained. Only the data for the β-anomeric forms of the oligomers are shown.

other minor peaks appear in all spectra. These may represent impurities or perhaps trapped conformational states of low probability. The overall trend is for the number of intense spectral lines to increase with DP as new types of environments for interior ring carbon atoms appear. Some of the new interior peaks cannot be positively assigned, in particular some of the C(2) peaks. The $(G_3)_4$ spectrum is the last in the series for which a new interior carbon resonance is clearly observed (at 72.3 ppm, see Figure 2). For $(G_3)_5$ no new resonances are observed, and carbon resonances from terminal rings, penultimate rings, and other rings near the ends of the molecule become barely discernible or lost. In pullulan itself, no terminal ring resonances are observable except for what is apparently a $C(5)_{1\alpha}$ resonance at 70.9 ppm (see Figure 2); here α denotes the α-anomeric configuration at the reducing end of the chain. The loss of terminal ring resonances from the pullulan spectrum results in the observed 18 intense spectral lines.

Important to the analysis of ^{13}C relaxation data is the ability to differentiate between interior carbon atom spectral lines and spectral lines from carbons in terminal residues. The spectral lines which we observed to be most uniquely characteristic of the chain interior are those found at 101.2, 100.7_3, 78.8, 78.4, and 72.3 ppm (see Figures 2 and 3). These five lines do not appear until the $(G_3)_3$ spectrum, where the line at 72.3 ppm is barely discernible as a shoulder peak. They become more intense in higher oligomers and in pullulan itself and are assigned respectively in $(G_3)_3$ to atoms $C(1)_5$, $C(1)_6$, $C(4)_4$, $C(4)_5$, and $C(5)_5$. All of the remaining 13 lines observed in pullulan persist in oligomers smaller than $(G_3)_3$ and therefore are not included among those which we refer to henceforth as the "interior" carbon atoms.

The ^{13}C NT_1 values are shown in Figure 3; relaxation times for β-anomer carbons and standard deviations of the exponential fits for all relaxation times are given in the supplementary material. All T_1 values were calculated by

an exponential least-squares fit of the inversion recovery data to the equation

$$I(\tau) = I_{eq} - C \exp(-\tau/T_1) \quad (1)$$

where $I(\tau)$ is the normalized intensity for delay time τ, I_{eq} is the normalized intensity after infinite delay time, C is a constant (theoretically $2 \times I_{eq}$ for a perfect 180° pulse), and T_1 is the spin–lattice relaxation time. Data for at least 7, and usually 10, delay times were used in the fit. All three parameters I_{eq}, C, and T_1 were treated as variables in the fitting algorithm. This helps to make the T_1 values insensitive to small errors in the 180° and 90° pulse widths.[27] The 90° pulse width was detd. to be 33.4 ± 1.5 μs. Variation of the pulse width had no significant effect on the measured T_1's in a repeated experiment with maltotetraose.

Experimental T_2 values are also shown in Figure 3. The T_2 values were calculated by an exponential least-squares fit of the data to the equation

$$I(\tau) = I_0 \exp(-\tau/T_2) \quad (2)$$

where $I(\tau)$ is the normalized intensity for delay time τ, τ is the delay time between the 90° pulse and the observed spin echo, I_0 is the intensity immediately following the 90° pulse, and T_2 is the experimental spin–spin relaxation time. Again, data for at least 7, and usually 10, delay times were used in the fit. Both I_0 and T_2 were treated as variables in the fitting algorithm. The time between refocusing 180° pulses was 10 ms or less for all experiments in order to minimize effects of translational diffusion on the measured T_2. The delay time τ was determined by the number of 180° refocusing pulses.

Although the Carr–Purcell–Meiboom–Gill pulse sequence with phase alternation corrects for both pulse imperfections and magnetic field inhomogeneities,[24] noise decoupling of protons causes an irreversible reduction in the measured ^{13}C T_2 values as compared to the true values.[25] This reduction occurs because "noise-decoupled" ^{13}C's are not truly decoupled in the strictest sense. The proton to which a given ^{13}C nucleus is attached is in a definite spin state until it absorbs a photon from the noise decoupler. Before absorption the ^{13}C is coupled to the proton. Even after the proton absorbs a photon from the noise decoupler, the ^{13}C nucleus is coupled to it, but this time the proton is in the opposite spin state. The ^{13}C resonance frequencies for the two proton-spin states (assuming a single bonded proton) are about 140–170 Hz apart,[28] but if the noise decoupling is intense enough, the two lines coalesce into a single seemingly sharp line without apparent scalar coupling, yielding the noise-decoupled spectrum.[29] However, because noise decoupling is incoherent, the intervals between successive proton flips are not equal, and each ^{13}C nuclear magnetic moment therefore takes a "random walk" around its resonant frequency. This results in an irreversible loss of phase for an ensemble of ^{13}C nuclei with the same chemical shift and thereby shortens the experimental T_2. This problem can be circumvented by using coherent decoupling,[30] but coherent decoupling is impractical for molecules with a wide range of ^{13}C chemical shifts such as saccharides.

Our approach to this problem is to calculate a corrected T_2, T_{2cor}. Because the same decoupling power was used in all experiments,[29] it is expected that the experimental T_2, T_{2exptl}, is related to T_{2cor} by the relation

$$1/T_{2exptl} = 1/T_{2cor} + 1/T_{2dcpl} \quad (3)$$

where T_{2dcpl} is the contribution due to noise decoupling. Since glucose is a small molecule, one expects to observe extreme narrowing, i.e., $T_1 = T_{2cor}$.[3-5] We assume that differences in the ^{13}C–^1H coupling constants of the different carbon atoms can be ignored, and use the average T_1 for the glucose resonances to calculate T_{2dcpl} = 1.35 s. Some T_{2cor} values are shown in Figures 4–8. The correction is only significant for $T_{2exptl} \geq 0.15$ s.

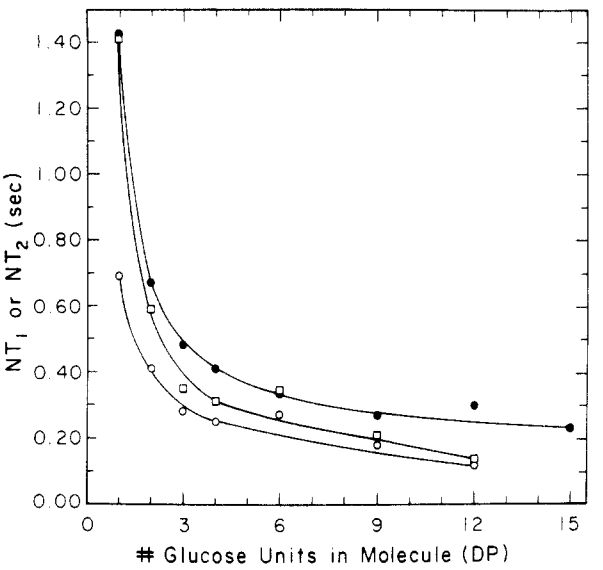

Figure 4. Average NT_1 (●), NT_{2exptl} (○), and NT_{2cor} (□) values of resolvable β-anomer reducing ring peaks as a function of the DP of the oligomers. N (the number of directly bonded hydrogen atoms) = 1 for C(1)–C(5) of each ring and 2 for C(6).

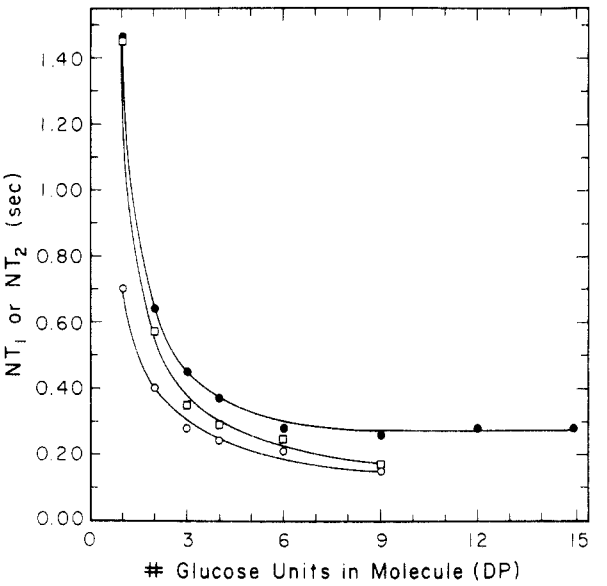

Figure 5. Average NT_1 (●), NT_{2exptl} (○), and NT_{2cor} (□) values of resolvable α-anomer reducing ring peaks as a function of the DP of the oligomers.

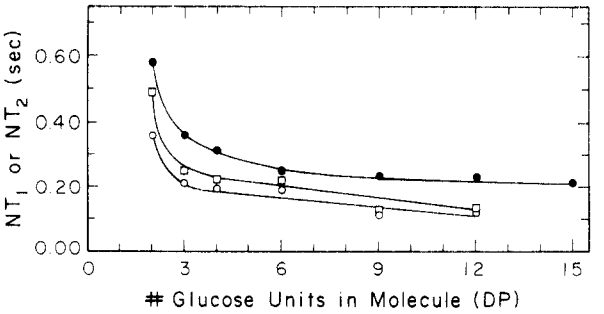

Figure 6. Average NT_1 (●), NT_{2exptl} (○), and NT_{2cor} (□) values of resolvable nonreducing end ring (opposite reducing ring) peaks as a function of the DP of the oligomers.

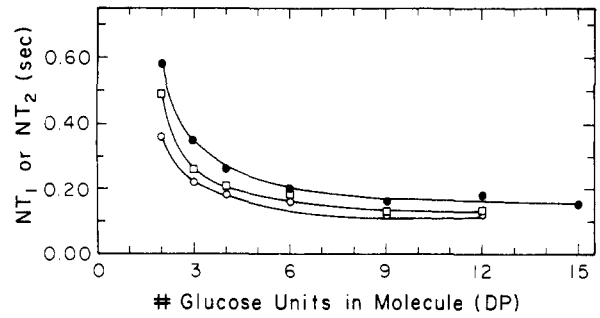

Figure 7. Average NT_1 (●), NT_{2exptl} (○), and NT_{2cor} (□) values of resolvable penultimate ring peaks as a function of the DP of the oligomers.

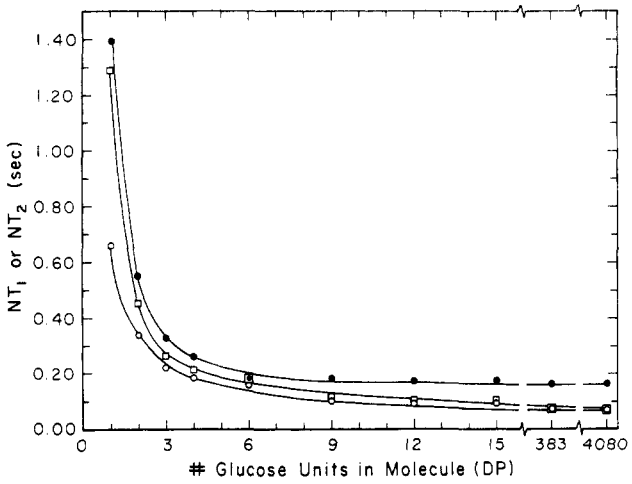

Figure 8. Average NT_1 (●), NT_{2exptl} (○), and NT_{2cor} (□) values for the interior carbon resonances of $(G_3)_3$, $(G_3)_4$, $(G_3)_5$, and pullulan or for the five resonances with the shortest NT_1 values for G_1, G_2, G_3, G_4, and $(G_3)_2$.

The NOE values (supplementary material) were determined from ratios of the peak intensities in the decoupled and gate-decoupled spectra for glucose, pullulan, $(G_3)_4$, and $(G_3)_5$. For all glucose resonances, the NOE was 2.9 ± 0.2, indicating dipolar relaxation as expected.[3-5] For pullulan, the NOE was 1.7 ± 0.2 for all resonances. For $(G_3)_4$ and $(G_3)_5$ the NOE varied significantly with the ring position, but the average of the five interior carbon resonances was 2.0 ± 0.2 for $(G_3)_4$ and 1.9 ± 0.2 for $(G_3)_5$.

Figure 3 shows how the experimental ^{13}C NT_1 and NT_2 values depend on the atom positions in the oligomers and polymer. Because of the superposition of many of the spectral lines, several carbon atoms in a given molecule can share the same measured NT_1 or NT_2 values. In these cases the experimental NT_1 and NT_2 values represent weighted averages of the NT_1 and NT_2 values of the several carbon atoms whose spectral lines overlap. Overall, the error is estimated to be ±10% for the T_1 values and ±20% for the T_2 values.

The ^{13}C relaxation is very similar for all carbon atoms (including C(6)) in a given ring, which suggests that the overall motion of the ring dominates the relaxation of all of its carbon atoms. Carbon atoms involved in glycosidic linkages exhibit the only significant exceptions to this observation. For example, C(4) atoms involved in α-1,4-linkages tend to have NT_1 values intermediate between the mean T_1 value for their own ring and that of the ring to which they are attached by the glycosidic linkage. Curiously, the α-1,4-linked $C(1)_2$ atoms in the various oligomers have anomalously low NT_1 values, apparently indicating less conformational freedom and molecular motion at this particular position. In the oligomers, but not in the polymer, C(6) atoms involved in α-1,6-linkages exhibit significantly lower NT_1 (and NT_2) values than do the unglycosylated C(6) atoms. As is the case for glucose, there is significantly more of the β-anomer than of the α-anomer at the reducing terminal of all oligomers.

The variation of NT_1 with ring number is more interesting. For all oligomers NT_1 values (and NT_2 values to a lesser extent) are significantly larger for the reducing residue than at the nonreducing terminus. It is tempting to surmise that the difference is due to the "extra motion" associated with the anomeric equilibrium at the reducing residue. For the longer oligomers (G_4 and higher) Figure 3 shows consistently larger NT_1 values for the reducing and nonreducing terminal rings than for the interior rings. It is surprising that the central ring of maltotriose, which has consistently higher NT_1 values (except for C(1)) than does the nonreducing-end residue, is an exception to this generalization based on the higher oligomers.

Except for terminal ring effects, the trends in NT_1 and NT_2 values as a function of carbon atom location within a given oligomer are subtle, often within the limit of experimental error. Much more striking are the trends in mean NT_1 and NT_2 values with increasing DP shown in Figures 4–8. Figure 4 shows the dependence on DP of the average NT_1 and NT_2 values of the carbons of the terminal β-anomer reducing rings. Figure 5 presents the same information for α-anomer reducing rings, Figure 6 for rings at the nonreducing terminus, and Figure 7 for the rings adjacent to the reducing end. Figure 8 shows the variation of the average NT_1 and NT_2 values for the interior carbon resonances of $(G_3)_3$, $(G_3)_4$, $(G_3)_5$, and pullulan; for the other oligomers Figure 8 gives the average NT_1 and NT_2 values for the five resonances with the smallest observed T_1 values. In all cases the NT_1 and NT_2 values of the oligomers approach an asymptotic limit at about DP = 12. Below this DP, the NT_1 and NT_2 values decrease toward this asymptote with increasing DP. If we define the critical DP as the DP for which the NT_1, NT_2, and NOE values of the interior carbon resonances are all within 10% of their values for pullulan, the critical DP is found to be 15, i.e., $(G_3)_5$. If definition of the critical DP is restricted to a consideration of only the NT_1 and NT_2 values, this criterion is met at DP = 12.

Even when an oligomer equals or exceeds the critical DP in length, the reducing and nonreducing terminal rings exhibit higher NT_1, NT_2, and NOE values than do the interior rings. This is also true for penultimate rings. Only the interior carbon atoms are "polymer matched" near the critical DP. It is interesting that polymer matching has not been observed for synthetic polymers until significantly higher DP's.[11] Part of the explanation for this is that the T_1's and T_2's for terminal groups, penultimate groups, and interior groups of the reported synthetic polymers occur at the same chemical shifts[31-33] so that the contributions from the longer relaxation times of the end groups do not become insignificant until higher DP's are reached. The advantage of using a series of oligomers with separate resonances for inner groups and end groups is clear: polymer matching can be observed for inner groups before the low concentrations of end groups render their contributions to a resonance line undetectable. The system of pullulan oligomers is not perfect in this regard, but at least it is possible to differentiate among the three glucose units closest to each chain end and those which are closer to the center of the oligomer.

The close match between the ^{13}C relaxation parameters (T_1, T_2, and NOE) of the interior carbons of $(G_3)_5$ and those of pullulan provides strong evidence that the local motion

of these atoms is very similar in both molecules. In $(G_3)_5$ the five interior carbon resonances represent three atoms each: $C(1)_{5,8,11}$, $C(1)_{6,9,12}$, $C(4)_{4,7,10}$, $C(4)_{5,8,11}$, and $C(5)_{5,8,11}$. It is probable that the carbon atoms in rings 4–6 and 10–12 have higher ^{13}C relaxation parameters than carbon atoms in rings 7–9 because the latter belong to the central G_3 unit whereas the former belong to the two penultimate G_3 units. The contributions from somewhat longer relaxation times for carbon atoms in penultimate G_3 units may explain the small difference between the interior carbon ^{13}C relaxation parameters of $(G_3)_5$ and pullulan although this difference is less than the experimental error for all parameters. It is striking that carbon atoms in the interior rings of pullulan oligomers only 12 or 15 rings in length have had their motions damped sufficiently to match atoms in pullulan molecules consisting of hundreds or thousands of sugar residues. It is our conclusion that the relative angular motion of these interior carbon atoms and their directly bonded H atoms generates the same spectral density of electromagnetic power at the pertinent magnetic resonance frequencies as the equivalent atoms in pullulan and that this implies that the underlying atomic motion is the same in both cases.

The sharp decreases in NT_1 and NT_2 in going from glucose to maltotetraose (Figures 4–8) may indicate that the α-1,4-linkages in the maltooligomers are stiff and allow little relative motion of the rings they connect. The rapid leveling off of the NT_1 and NT_2 values observed for the pullulan oligomers is consistent with the notion based on conformational analysis[15,34] that α-1,6-linkages permit greater relative motion of the maltotriose units they join. Further considerations of the relative conformational freedom of 1,4- and 1,6-glycosidic linkages may permit a more quantitative interpretation of the present results.

Acknowledgment. We thank Dr. Rudi Nunlist for calling our attention to the effect of noise decoupling on measured T_2 values and Dr. Shoumo Chang for advice on an effective means for elminating O_2 from aqueous solutions. This work has been supported by NIH Research Grant GM 33062.

Supplementary Material Available: Table I containing ^{13}C chemical shifts, T_1 and T_2 with the standard deviations of their exponential fits, and NOE values (when determined) for all molecules (13 pages). Ordering information is given on any current masthead page.

References and Notes

(1) E. O. Stejskal and J. E. Tanner, *J. Chem. Phys.*, **42**, 288 (1965).
(2) P. Stilbs, *J. Colloid Interface Sci.*, **87**, 385 (1982).
(3) W. T. Huntress, *Adv. Magn. Reson.*, **4**, 1 (1970).
(4) D. Doddrell, V. Glushko, and A. Allerhand, *J. Chem. Phys.*, **56**, 3683 (1972).
(5) D. E. Woessner, *J. Chem. Phys.*, **36**, 1 (1962).
(6) J. R. Lyerla, H. M. McIntyre, and D. A. Torchia, *Macromolecules*, **7**, 11 (1974).
(7) D. A. Torchia and J. R. Lyerla, *Biopolymers*, **13**, 97 (1974).
(8) S. Berger, F. R. Kreissel, D. M. Grant, and J. D. Roberts, *J. Am. Chem. Soc.*, **97**, 1805 (1975).
(9) M. Vignon, F. Michon, J. Joseleau, and K. Bock, *Macromolecules*, **16**, 835 (1983).
(10) G. C. Levy, D. J. Craick, A. Kumar, and R. E. London, *Biopolymers*, **22**, 2703 (1983).
(11) F. Heatley, *Prog. Nucl. Magn. Reson. Spectrosc.*, **13**, 47 (1979).
(12) J. Skolnick, D. Perchak, and R. Yaris, *J. Magn. Reson.*, **57**, 204 (1984).
(13) A. Benesi and J. T. Gerig, *Carbohydr. Res.*, **53**, 278 (1977).
(14) K. Matsuo, *Macromolecules*, **17**, 449 (1984).
(15) B. A. Burton and D. A. Brant, *Biopolymers*, **22**, 1769 (1983).
(16) T. Kato, T. Okamoto, T. Tokuya, and A. Takahashi, *Biopolymers*, **21**, 1623 (1982).
(17) K. Wallenfels, G. Keilich, G. Bechtler, and D. Freudenberger, *Biochem. Z.*, **341**, 433 (1965).
(18) G. S. Drummond, E. E. Smith, and W. J. Whelan, *FEBS Lett.*, **5**, 85 (1969).
(19) G. A. Morris and L. D. Hall, *Can. J. Chem.*, **60**, 2431 (1982).
(20) A. Heyraud, M. Rinaudo, M. Vignon, and M. Vincendon, *Biopolymers*, **18**, 167 (1979).
(21) P. Colson, H. J. Jennings, and I. C. P. Smith, *J. Am. Chem. Soc.*, **96**, 8081 (1974).
(22) M. John, G. Trenel, and H. Dellweg, *J. Chromatogr.*, **42**, 476 (1969).
(23) K. Kainuma, A. Nogama, and C. Mercier, *J. Chromatogr.*, **121**, 361 (1976).
(24) R. Freeman and S. Wittekoek, *Proc. Colloq. AMPERE*, **15**, 205 (1969).
(25) R. Freeman and H. D. W. Hill in "Dynamic Nuclear Magnetic Resonance Spectroscopy", L. M. Jackman and F. A. Cotton, Eds., Academic Press, New York, 1975, Chapter 5, pp 131–62.
(26) R. K. Harris and R. H. Newman, *J. Magn. Reson.*, **24**, 449 (1976).
(27) Bruker Instruments, Inc., personal communication.
(28) A. S. Perlin and B. Casu, *Tetrahedron Lett.*, **34**, 2921 (1969).
(29) R. R. Ernst, *J. Chem. Phys.*, **45**, 3845 (1966).
(30) R. Freeman and H. D. W. Hill, *J. Chem. Phys.*, **54**, 3367 (1971).
(31) K. J. Liu and R. Ullman, *J. Chem. Phys.*, **48**, 1158 (1968).
(32) V. Inome, A. Nishioka, and R. Chujo, *J. Polym. Sci., Polym. Phys. Ed.*, **11**, 2237 (1973).
(33) C. Cuniberti, *J. Polym. Sci., Part A-2*, **8**, 2051 (1970).
(34) A. Allerhand and R. K. Hailstone, *J. Chem. Phys.*, **56**, 3718 (1972).
(35) D. A. Brant and B. A. Burton in "Solution Properties of Polysaccharides", D. A. Brant, Ed., American Chemical Society, Washington, DC, 1981, ACS Symp. Ser. No. 150, Chapter 7.